

UC Berkeley

Indoor Environmental Quality (IEQ)

Title

Convective and radiative heat transfer coefficients for individual human body segments

Permalink

<https://escholarship.org/uc/item/9hn3s947>

Authors

de Dear, Richard J.
Arens, Edward A
Zhang, Hui, Ph.D
et al.

Publication Date

1996-11-27

Peer reviewed

Richard J. de Dear · Edward Arens · Zhang Hui
Masayuki Oguro

Convective and radiative heat transfer coefficients for individual human body segments

Received: 21 May 1996/Accepted: 27 November 1996

Abstract Human thermal physiological and comfort models will soon be able to simulate both transient and spatial inhomogeneities in the thermal environment. With this increasing detail comes the need for anatomically specific convective and radiative heat transfer coefficients for the human body. The present study used an articulated thermal manikin with 16 body segments (head, chest, back, upper arms, forearms, hands, pelvis, upper legs, lower legs, feet) to generate radiative heat transfer coefficients as well as natural- and forced-mode convective coefficients. The tests were conducted across a range of wind speeds from still air to 5.0 m/s, representing atmospheric conditions typical of both indoors and outdoors. Both standing and seated postures were investigated, as were eight different wind azimuth angles. The radiative heat transfer coefficient measured for the whole-body was 4.5 W/m² per K for both the seated and standing cases, closely matching the generally accepted whole-body value of 4.7 W/m² per K. Similarly, the whole-body natural convection coefficient for the manikin fell within the mid-range of previously published values at 3.4 and 3.3 W/m² per K when standing and seated respectively. In the forced convective regime, heat transfer coefficients were higher for hands, feet and peripheral limbs compared to the central torso region. Wind direction had little effect on convective heat transfers from individual body segments. A general-purpose forced convection equation suitable for application to both seated and standing postures indoors was $h_c = 10.3v^{0.6}$ for the whole-body. Similar equations were generated for individual body segments in both seated and standing postures.

Key words Convection · Radiation · Heat transfer coefficient · Thermal manikin · Thermal comfort

Introduction

The various avenues of energy exchange between the human body and its thermal environment have been quantified by diverse disciplines concerned with human thermal tolerance and comfort, including physiology, engineering, architecture, psychology and meteorology (Nishi and Gagge 1970). A goal for comfort and heat stress research is a comprehensive model of human thermoregulation and prediction of thermal comfort by numerical algorithms. The model needs to be anatomically detailed, and able to distinguish the effects of spatial and temporal changes of conditions around the body. The completion of such a model depends partly on obtaining empirically verified heat transfer coefficients at the scale of individual body segments such as arms, legs, head and hands.

Two potential users of a detailed model would be the auto/transportation industry and the heating, ventilating and air-conditioning (HVAC) industry. Recently developed task/ambient air-conditioning systems provide personalized microclimatic controls for individual workers (Heinemeier et al. 1990). These systems function by creating highly asymmetric or non-isothermal environments around the workstation (Bauman et al. 1993), including vertical temperature gradients, radiant asymmetries and highly non-uniform airflow regimes directed at specific body regions such as the head, chest, or back. By deliberately departing from the conventional goal of (HVAC) practice of isothermal, low-speed air flow uniformity within the entire room, task/ambient conditioning designs have highlighted the shortcomings of earlier numerical models of human thermal balance and thermoregulation. Examples are the Predicted Mean Vote (PMV; Fanger 1970) and Pierce 2-node models (Gagge et al. 1986), which resolve all heat and mass fluxes only at the whole-body level.

R.J. de Dear (✉)
Climatic Impacts Centre, Macquarie University, Sydney,
NSW 2109, Australia

E. Arens · Z. Hui
Centre for Environmental Design Research, 390 Wurster Hall,
University of California, Berkeley, CA 94720, USA

M. Oguro
Taisei Corporation, 344-1. Nase-cho, Totsuka-ku, Yokohama 245,
Japan

The first attempts at multimode human thermal simulations as opposed to whole-body analyses (e.g. Stolwijk 1970; Wissler 1970; Houdas 1981) resorted to segmentation of the human body into simple geometric shapes, such as cylinders and spheres, in order to use heat and mass transfer data established for such shapes in the engineering literature. More recently, however, articulated thermal manikins have enabled much improved anatomical resolution of the human form (Tanabe et al. 1994; Wyon 1989).

The purpose of this paper is to report convective and radiative heat transfer coefficients for individual body segments as represented by a realistic-looking human thermal manikin consisting of 16 discrete anatomical segments. The unclothed manikin was exposed to a wide range of microclimatic conditions, typical of both indoor and outdoor situations, which were produced within a climate chamber and a boundary layer wind tunnel. The paper summarizes the findings into radiative heat transfer coefficients (h_r), natural convective heat transfer coefficients (h_c), and empirically fitted regression functions of the dependence of h_c on air speed (v).

The following main factors in the design of this research are included.

1. Wind speed: the range must cover both indoor and outdoor conditions and encompass natural (free), mixed mode, and forced convective regimes. The tests therefore range from still air conditions ($v < 0.1$ m/s) to the start of forced convection (≈ 0.2 m/s) and up to 5 m/s, equivalent to moderate outdoor wind.
2. Wind direction: applications such as task/ambient conditioning require information on air flows directed at the body from a variety of angles. The paper investigates eight wind directions, starting with 0° (facing into the wind), 45° , 90° (right-side), 135° , 180° (back to the wind), 225° , 270° (left-side) and 315° .
3. Posture: both seated and standing postures are examined.

Basic physics of body dry heat transfer

The influential ASHRAE Handbook of Fundamentals (1993) partitions total dry heat transfer to and from the human body into convective and radiative fluxes:

$$C = f_{cl} h_c (t_{cl} - t_a) \quad (\text{W/m}^2)$$

and

$$R = f_{cl} h_r (t_{cl} - \bar{t}_r) \quad (\text{W/m}^2)$$

where h_c is the convective heat transfer coefficient (W/m^2 per K); h_r is the linear radiative heat transfer coefficient (W/m^2 per K); f_{cl} is the clothing area factor, representing the ratio of clothed body surface area to nude body surface area (A_{cl}/A_b) and approximated as $1 + 0.3 I_{cl}$ for an ensemble, with I_{cl} being the intrinsic clothing ensemble insulation in clo ($f_{cl} = \text{unity}$ for the nude situation); t_{cl} is the clothed body's mean surface temperature ($^\circ\text{C}$);

t_a is the ambient air temperature ($^\circ\text{C}$); and \bar{t}_r is mean radiant temperature perceived by the body ($^\circ\text{C}$).

While the present paper is not directly concerned with evaporative heat fluxes, the modified Lewis relation will allow the current convective heat transfer coefficients in air to be used in the prediction of evaporative heat transfers, which are important in most heat balance models and thermal strain indices (Nishi and Gagge 1970). According to the ASHRAE Handbook of Fundamentals (1993), the Lewis relation (LR) can be defined simply as the ratio of evaporative and convective heat transfer coefficients (h_e/h_c) and is approximately equal to 16.5 K/kPa at sea-level atmospheric pressures (ASHRAE 1993).

Radiative heat transfer coefficient (h_r)

The ASHRAE Handbook of Fundamentals (1993) indicates that the linearized radiative heat transfer coefficient (h_r) can be calculated from:

$$h_r = 4\varepsilon\sigma(A_r/A_D)[273.2 + (t_{cl} + \bar{t}_r)/2]^3 \quad (\text{W/m}^2 \text{ per K})$$

where ε is the average body surface emissivity (ND); σ is the Stefan-Boltzmann constant, $5.67 \cdot 10^{-8}$ W/m^2 per K; A_D is the DuBois body surface area (m^2); A_r is the effective radiation area of the human body (m^2); t_{cl} is the average clothed body surface temperature ($^\circ\text{C}$); \bar{t}_r is the mean radiant temperature of the environment ($^\circ\text{C}$).

While estimates for A_r/A_D for the nude body are available in the literature (0.70 and 0.73 for sitting and standing respectively; Fanger 1970), and emissivity can reasonably be assumed to equal 0.95, explicit solutions for h_r are rarely obtained for clothed subjects due to the difficulties in measuring t_{cl} . Therefore the value $h_r = 4.7$ W/m^2 per K has been widely accepted as a reasonable whole-body estimate for general purposes (ASHRAE 1993).

Since individual body segments such as arms, legs and trunk have diverse dimensional characteristics, Stolwijk's 25-node model of human thermoregulation (Stolwijk 1970) applied conventional engineering estimation techniques to derive convective and radiative heat transfer coefficients for individual body segments (Table 1). Ichihara et al. (1995) recently used an articulated thermal manikin with 16 body segments in a novel approach to the separation of anatomically specific convec-

Table 1 Stolwijk's estimated radiative heat transfer coefficients for simple geometric representations of human body segments (Stolwijk 1970)

Segment	Assumed shape	Radiative heat transfer coefficient (W/m^2 per K)
Head	Sphere	6.40
Trunk	Cylinder	5.24
Arms	Cylinder	5.24
Hands	Cylinder	3.49
Legs	Cylinder	5.24
Feet	Cylinder	4.65

Table 2 Ichihara estimates of body segment h_r for a standing thermal manikin with $\epsilon=0.96$ (Ichihara et al. 1995)

Segment	Radiative heat transfer coefficient (W/m ² per K)
Head	4.3
Chest	3.8
Upper arm/shoulder	4.0
Back	3.6
Pelvis	3.9
Forearms	3.9
Hands	3.7
Thighs	4.2
Lower legs	4.8
Feet	7.3

tive and radiative fluxes. The instrument had its mean skin temperature actively regulated to equal air temperature within a climate chamber ($t_a=t_{sk}=34$ °C), thereby cancelling any convective heat exchanges between manikin and environment and equating total dry heat loss ($C+R$) to just R . The climate chamber surface temperatures were independently controlled to give mean radiant temperatures of 27.0 and 28.1 °C. The resulting h_r estimates, segment-by-segment, are listed in Table 2.

The anomalously high values of h_r found however for segments closest to the floor, such as feet and lower legs, possibly reflect the influence of thermal stratification within the climate chamber. The areally weighted average h_r from this experiment was 4.3 W/m² per K, a value in reasonably good agreement with the whole-body value of 4.7 W/m² per K which is widely accepted in the literature (ASHRAE 1993).

Nevertheless, the true areally weighted average would be significantly below 4.7 W/m² per K were the leg and feet h_r values not overestimated because of thermal stratification.

Convective heat transfer coefficient (h_c)

Convective heat transfer from skin or clothing results from an airstream perturbing the insulating boundary layer of air clinging to the surface of the body. Generally, the faster the flow of air around the body, the thinner the boundary layer of air on the body's surface, and hence the lower the thermal insulation afforded the subject. The process of convection from a heated surface such as human skin or clothing can be further classified into three distinct modes: natural convection, where the air movement is driven purely by thermally induced buoyancy and generally confined to ambient air speeds lower than 0.2 m/s; forced convection at speeds generally higher than $c.$ 1.5 m/s (Danielsson 1993), and a region of mixed-mode convection prevailing at air speeds between these two limits.

The fundamental nondimensional quantities describing forced convection are Nusselt number (Nu), Prandtl number (Pr) and Reynolds number (Re). These can be expressed as follows:

$$Nu=h_c d/k$$

$$Pr=\nu/\alpha$$

$$Re=\nu d/\nu$$

where h_c is the convective heat transfer coefficient (W/m² per K); k is thermal conductivity of the fluid ($k=0.0267$ W/m per K for air at 20 °C); d is the characteristic dimension of the body or segment in question such as diameter of cylindrical segments (m); ν is air speed (m/s); ν is kinematic viscosity (m²/s); and α is thermal diffusivity (m²/s).

These three dimensionless groups can be related together with the following equation:

$$Nu=KPr^a Re^b$$

where K is a constant and a and b are empirical exponents. Since Pr is relatively static at 0.72 across the temperature range 10–50 °C, Nishi and Gagge (1970) indicate that the above relation can be simplified to:

$$Nu=CRe^b$$

Appropriate values for C and b in the range $400 < Re < 4000$ are 0.615 and 0.466 respectively, while C and b in the range $4000 < Re < 40000$ correspond to 0.174 and 0.618 respectively (Nishi and Gagge 1970).

Fanger's PMV model (1970) supplies a widely accepted approximation for h_c for the human body under natural convection:

$$h_c=2.38(t_{cl}-t_a)^{0.25} \quad (\text{W/m}^2 \text{ per K})$$

which indicates a value of ≈ 3.6 W/m² per K for typical indoor situations with a 5 K temperature gradient between body and environment. To date, this probably stands as the most frequently adopted value in numerical modelling of human heat transfer at the whole-body level. Surface convective heat fluxes in Stolwijk's 25-node model of human thermoregulation (1970) were based on the engineering literature for cylinders and spheres. A summary of those data for natural convection is provided in Table 3.

Three fundamentally different approaches have been applied to the study of convection of the human body surface at wind speeds greater than $c.$ 0.2 m/s. The first involves the use of heat flux sensors on the surface of the body (e.g. Danielsson 1993; Clark and Toy 1975). The principle of these devices is the separation of two known temperatures by a known thermal resistance. That is, two temperature sensing devices, usually embedded into flat discs of about 3 cm diameter, are arranged face-to-face, but with a small thickness, say 1.5 mm, of known thermal resistance between them. Assuming the two discs achieve an equilibrium temperature corresponding to the medium or surface in which they are suspended or attached to, the temperature gradient between the two discs divided by the known resistance separating them approximates the net heat flux through the instrument. In order to eliminate the radiant component of the disks' surface heat balance, Danielsson (1993) covered the device with aluminum foil with emissivity (ϵ) assumed to be 0.04. The advantage of the heat flux plate approach is

Table 3 Stolwijk's assumed natural convective heat transfer coefficients for simple geometric representations of human body segments (Stolwijk 1970)

Segment	Assumed shape	Characteristic length (m)	Characteristic radius (m)	Natural convective heat transfer coefficient (W/m ² per K)
Head	Sphere		0.105	0.66
Trunk	Cylinder	0.60	0.142	1.86
Arms	Cylinder	1.12	0.044	3.95
Hands	Cylinder	0.96	0.015	6.05
Legs	Cylinder	1.60	0.064	3.61
Feet	Cylinder	1.25	0.016	5.93

(Area weighted average=3.37)

that spot values at any point across the body's complex morphology can be measured and that human subjects in motion can be used, although whole segment, or indeed, whole body averages require a large number of spot values to be assessed. The main disadvantage was stated by Danielsson (1993) to be that the instrument itself interferes with the air flow around the body as well as the temperature of the surface to which it is attached.

The second approach to measuring convection is based on the use of the rate of naphthalene sublimation as a surrogate for the process of convective heat transfer (Nishi and Gagge 1970; Chang et al. 1988). The amount of weight lost by the naphthalene through sublimation into the atmosphere is translated into convective heat loss by use of the Chilton-Coburn analogy between heat and mass transfer. Chang et al. (1988) applied circular naphthalene disks into the surface of various body segments on an articulated manikin in a wind tunnel to assess the walking-induced 'pendulum effect' (Clark and Edholm 1985). The main disadvantage of this approach is the laborious experimental technique required and the spot nature of the results.

The third approach uses a manikin with controlled skin temperature (Tanabe et al. 1994; Wyon 1989). Because the heat flux measurements are done by circuitry actually embedded within the 'skin,' they are less obtrusive and therefore more accurate than the surface heat flux technique. Another important advantage of the method is that its measurements are made across the entire surface area, as opposed to spot locations, thus ensuring very accurate spatial averages for individual segments, or the whole body. The main disadvantage of the manikin technique is the absence of realistic body motion that only human subjects can provide. However, there have been attempts to overcome this shortcoming with the use of articulated manikins, which can be made to 'walk' on a treadmill or 'pedal' an ergometer (e.g. Olesen et al. 1982; Chang et al. 1988). The present study is not concerned with body motion or the pendulum effect.

Many attempts have been made over the years to empirically define forced convective heat transfer coefficients appropriate for the whole human body. The general form of the equation describing the dependence of whole body h_c on air speed, v , is as follows:

$$h_c = Bv^n \quad (\text{W/m}^2 \text{ per K})$$

with most authors indicating n in the region of 0.5 to 0.6. Kerslake (1972), and subsequently McIntyre (1980) recommended a value of $B \approx 8.3$ and exponent $n = 0.5$, which is not appreciably different from the equation used by Gagge et al. (1986) in the 2-node model of human thermoregulation, based on a subject walking through still air at speed v :

$$h_c = 8.6\sqrt{v} \quad (\text{W/m}^2 \text{ per K})$$

Fanger's widely used PMV model (Fanger 1970), however, is based on a significantly larger estimate from the work of Winslow et al. (1939) on semi-reclining subjects exposed to downdrafts:

$$h_c = 12.1\sqrt{v} \quad (\text{W/m}^2 \text{ per K})$$

while Seppänen's (1972) estimate for a standing subject in moving air ranks among the highest in the literature to date [presented in ASHRAE (1993, p 8.9) on the basis of data published by Seppänen et al. (1972)]:

$$h_c = 14.8v^{0.69} \quad (\text{W/m}^2 \text{ per K})$$

Under natural convection in still air, it is to be expected that different body segments will have varying rates of heat loss because of the different flow regimes at differing heights from the leading edge. The natural convective boundary layer flow may be characterized as either laminar or turbulent, and the non-dimensional (ND) Grashof number (Gr) describes the transition from former to latter in terms of the ratio of buoyancy forces to viscous forces (Clark 1981):

$$Gr = \frac{g h^3 (T_{sk} - T_a)}{\nu^2 T_a} \quad (\text{ND})$$

where g is the acceleration due to gravity (9.8 m/s²); h is the vertical height of the body (m); ν is the kinematic viscosity of air (m²/s); T_{sk} is absolute skin temperature (K); and T_a is absolute air temperature (K).

Generally, when $Gr < 10^8$ the flow is laminar, and when $Gr > 10^{10}$ the flow is turbulent. Clark and Toy (1975) indicate that a laminar flow regime applies up to a height of about 0.8 m for a standing, nude human form with $T_{sk} = 306$ and $T_a = 298$ K.

Convective heat transfer from individual body sites can be expected to vary in the horizontal plane as well.

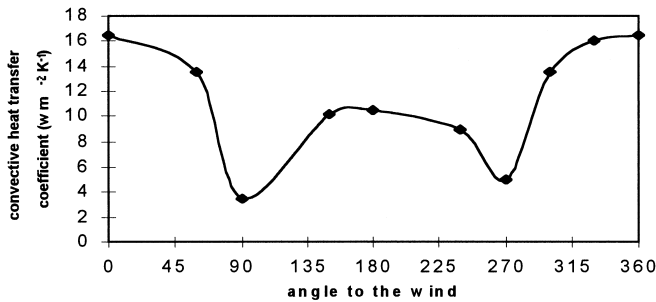


Fig. 1 Convective heat transfer coefficients measured with a small surface plate calorimeter attached to different points on the human head immersed in a 0.8 m/s wind blowing onto the face (0°) (after Clark and Toy 1975)

McIntyre (1980) indicates that it is highest for those parts of the body facing directly into the wind and also high for the leeward side of the body or limb, while the coefficient is smallest across the transverse axis of the body or limb. Using a mean air speed of 0.47 m/s directed at the face of a heated manikin head, Mayer (1992) found $h_c=10.5$ W/m² per K for the forehead, 1.5 at the sides of the head, 11.0 on the crown and 5.5 W/m² per K at the back of the neck. Similar findings were presented earlier by Clark and Toy (1975) who also directed an air stream onto the face of a heated manikin head and measured heat flux with a small heat flux plate (see Fig. 1). Danielsson (1993) used small heat flux plates attached to different locations around individual body segments to determine local convective heat transfer coefficients. Natural convective heat transfer coefficients were generally in the range 4 to 6 W/m² per K.

Methods

The basic approach adopted in the present study involved the use of a skin-temperature-controlled manikin exposed to a variety of precisely regulated wind speeds within a boundary layer wind tunnel. The manikin simultaneously measures total dry heat transfer from its surface and the corresponding skin temperature. Coupled with simultaneous measurements of operative temperature in the environment, the manikin's surface heat loss can be partitioned into convective and radiative components by assuming that $t_a=t_r$ within the working section of the wind tunnel.

Thermal manikin – 'Monika'

Wyon (1989) has reviewed both the general theory and practical applications of thermal manikins. The manikin used for the current experiments is described in detail elsewhere (Tanabe et al. 1994). Suffice it to say the manikin resembles a female show-room dummy (named 'Monika'), which has 16 independent body segments, each consisting of a 4-mm-thick fibre-glass armed polyester shell covered with 0.3 mm nickel wire wound at a spacing of 2 mm to ensure even heating across the entire surface area of the instrument. Although the nickel wire is covered with a protective skin of 0.1 to 1.0 mm thickness, the proximity of the nickel heating element to the surface confers a very short time constant on the manikin. The time constant is further improved by the use of the same nickel winding for heating, measuring and controlling skin temperature functions of the manikin.

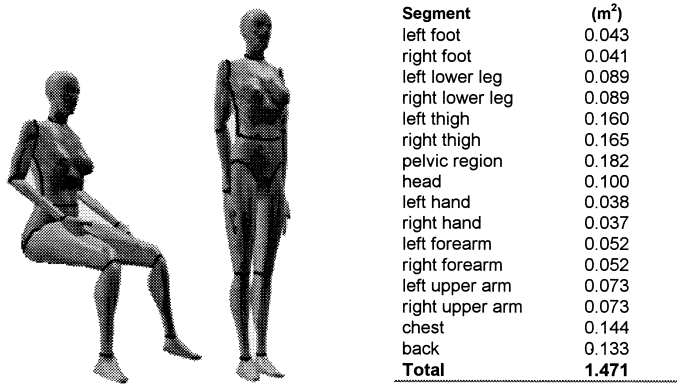


Fig. 2 The manikin's segmentation, surface areal dimensions and the two postures investigated in this study

Figure 2 gives an indication of the thermal manikin's segmentation and the basic areal dimensions of each body segment. Not indicated in Fig. 2 is the manikin's shoulder-length hair, which can be expected to reduce dry heat losses from the head/neck region considerably. The body-segmentation enables the manikin to assume a variety of postures, two of which were the focus of the present investigation. These were standing and seated, as depicted in Fig. 2 (note that the images are computer generated and not of the actual manikin). In the case of the seated experiments, the manikin was arranged in a simple wire-frame garden chair which has previously been demonstrated to exert minimal influence on convective heat loss.

Each of the 16 body segments is independently controlled by an external PC working on the principle that, under steady-state conditions, the heat supplied to each segment's nickel heating element is the same as the heat lost from skin to environment. Since the former is monitored constantly, as are the segment's surface (skin) temperature and the ambient environmental temperature, all data necessary for describing the segment's total dry heat balance are available.

The boundary layer wind tunnel

The wind tunnel used in these experiments is located in the Centre for Environmental Design Research, University of California at Berkeley, and is approx. 16 m long from air intake to working section. The working section of the facility did not allow the full-scale thermal manikin to stand fully erect, and this necessitated some adjustments to the experimental procedures (see subsequent paragraph entitled Procedures). The up-wind section for the wind tunnel was stripped bare of all roughness elements to be able to create an approximately uniform boundary layer wind speed profile between the manikin's feet and head during the experiments. The one exception to this was the placement of a large cylindrical drum (1.5 m tall and 0.5 m diameter) about 7 m up-wind on the floor of the tunnel in order to generate some large-scale eddies within the windflow.

Wind tunnel anemometry

Wind speeds were measured with a TSI (model 1266) heated element anemometer calibrated just prior to the experiments. The device ranges from 0.15 to 66 m/s with a specified error of $\pm 10\%$ at 0.2 and $\pm 2\%$ at 5.0 m/s. The anemometer was suspended in the air stream by a vertical mast which was driven by a programmable stepper-motor, enabling automatic wind speed profiles from floor to ceiling to be determined during each experiment. The anemometer mast's stepper motor was programmed to pause for 30 s at equally spaced heights, and the arithmetic average of 450 instanta-

Table 4 Anemometer heights used for each of the manikin's body segments

Manikin segment	Anemometer heights for the manikin's seated posture (m)	Anemometer heights for the manikin's standing posture (m)
Left foot	0.15	0.15
Right foot	0.15	0.15
left lower leg	Average of 0.28 and 0.41	Average of 0.28 and 0.41
Right lower leg	Average of 0.28 and 0.41	Average of 0.28 and 0.41
Left thigh	0.54	Average of 0.41, 0.54 and 0.66
Right thigh	0.54	Average of 0.41, 0.54 and 0.66
Pelvic region	0.66	Average of 0.66 and 0.79
Head	Average of 1.05 and 1.18	1.42
Left hand	0.66	0.54
Right hand	0.66	0.54
Left forearm	Average of 0.66 and 0.79	Average of 0.66 and 0.79
Right forearm	Average of 0.66 and 0.79	Average of 0.66 and 0.79
Left upper arm	0.92	Average of 0.92, 1.05 and 1.18
Right upper arm	0.92	Average of 0.92, 1.05 and 1.18
Chest	Average of 0.79 and 0.92	Average of 0.92, 1.05 and 1.18
Back	Average of 0.79 and 0.92	Average of 0.92, 1.05 and 1.18

neous speeds recorded during each of these pauses was sent out to the wind tunnel's datalogger. These averages recorded during each manikin exposure were the basis of subsequent convective heat transfer coefficient calculations. There were 11 separate anemometer measurements for a full sweep of the boundary layer. Their heights above the floor of the wind tunnel were: 0.02, 0.15, 0.28, 0.41, 0.54, 0.66, 0.79, 0.92, 1.05, 1.18 and 1.42 m. The data of Table 4 indicate those anemometer heights associated with each of the manikin's 16 body segments during both seated and standing experiments. Where more than one anemometer height is given in Table 4, the mean values obtained at adjacent measurement points were used.

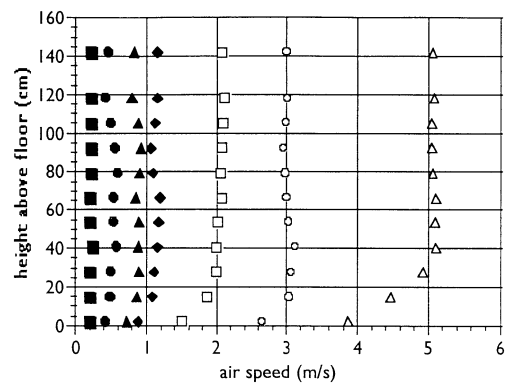
Airflow characteristics for the forced convection heat transfer experiments

The range of air speeds selected for investigation in the wind tunnel (0.2–5.0 m/s) was intended to provide forced convective heat transfer coefficients applicable in both indoor and outdoor contexts. While the upper limit of 5 m/s may look lower than many outdoor measurements, it is worth noting that outdoor meteorological stations typically record wind speeds at a height of 10 m above ground level. The boundary layer's logarithmic wind speed profile means that a value of 5 m/s at 1.5 m height, as studied in the present experiment, would occur with winds of ≥ 15 m/s at 10 m above ground level (Oke 1987).

Typical profiles within the wind tunnel's working section for the target wind speeds: 0.2, 0.5, 0.8, 1.2, 2, 3, and 5 m/s, are depicted in Fig. 3. The anemometer at 2 cm appeared to be the most affected by the floor's roughness, but this value can be disregarded since such a height was not used in any of the h_c calculations (see Table 4). The measurements at 15 and 28 cm above the floor were also marginally below the design speeds, underlining the importance of using actual anemometer readings rather than design speeds in all h_c calculations.

The turbulence produced in the tunnel by the upwind cylinder had an eddy size distribution similar to those found both indoors and outdoors, but the intensity of turbulence was lower than is typically found in occupied indoor environments. A power spectrum of the turbulent frequencies in the tunnel measured at a mean velocity of 2.35 m/s indicated an average eddy size of 0.77 m, which is appropriate for built environments. Mean values of Tu (across all heights) for the seven air speeds tested ranged from 4.1 to 8.4%.

Turbulence is known to influence convective heat transfer from heated surfaces (Test et al. 1981). Using a heat flux plate on the front of a human manikin's head, Mayer (1992) established that turbulence intensities (Tu , defined as the ratio of the standard deviation and mean of the instantaneous speeds) between 5 and 40%

**Fig. 3** Typical wind speed profiles measured during the h_c experiments

had a negligible effect across a velocity range from still air to 0.5 m/s air flow. However, he found that higher Tu values in the region of 70% increased h_c from 10 to 12 W/m² per K at a mean velocity of 0.5 m/s. In this experiment, the turbulence intensities were well below the levels found by Mayer (1992) to influence convective heat transfer.

Wind tunnel temperature sensors

Four temperature probes mounted at different heights on a mast within the wind tunnel's working section and near the manikin were continuously scanned and averaged by an automatic datalogger for 3 min during the final stages of each experiment. The probes were thermistors mounted at the tips of 30-cm-long shafts. The four measuring heights were selected to span the full height of the manikin's occupied zone within the wind tunnel's working section. All subsequent calculations performed on each manikin body segment were based on the closest of the four temperature probes.

Although the wind tunnel had no capability for temperature control, the variation of temperatures within the working sections was found to be negligible for the duration of a single manikin experiment (typically ± 0.15 K during a 1 h experiment). Furthermore, since all experiments were performed in low levels of illumination, the mean radiant temperature was found to be, for all intents and purposes, identical to air temperatures ($\Delta T < 0.15$ K) within the manikin's occupied zone.

Estimation of the radiative heat transfer coefficient

Since the manikin used by Ichihara et al. (1995) resembled closely that used in the current experiments, it would have been convenient to adopt their estimates of the 16 body segments' radiative heat transfer coefficients (Table 2). However, because of the difficulties experienced with vertical air temperature gradients in their study, an alternative approach was adopted here. Starting from Stefan's law of thermal radiation:

$$R = \epsilon \sigma T^4 \quad (\text{W/m}^2)$$

where R is radiant flux density (W/m^2); ϵ is emissivity of the surface (fraction, black body is W/m^2 per K unity); σ is Stefan-Boltzmann coefficient ($5.67 \cdot 10^{-8} \text{ W/m}^2$ per K); and T is absolute temperature of the emitter (K).

As $\epsilon \rightarrow 0$ then so does $R \rightarrow 0$. A simple strategy for isolating the convective component of the total dry heat transfer of the manikin is to cover the surface of the manikin with a very low emissivity (ϵ) coating. By removing most of the radiant component, the total heat transfer coefficient of the coated manikin becomes almost exclusively convective heat transfer.

Common aluminum cooking foil with an assumed ϵ of 0.10 (ASHRAE 1993, p 36.3) was applied tightly to the manikin with a very sparse sprinkling of gum adhesive. By ensuring a very tight fit between the low ϵ coating and the manikin, the risk of increasing thermal insulation by entrapped air was minimized. The efficacy of this approach was checked by inspecting the surface of the foil-covered manikin for spatial temperature gradients with a high-resolution thermographic camera (Inframetrics model 760). The emissivity of the uncoated (nude) surface was measured to be 0.95 by comparison with a reference surface of known emissivity.

To determine h_r for a given body segment, its total dry heat transfer was first measured with the foil in place ($h_{r(\text{foil})}$). These data were then compared with the total dry heat transfer ($h_{r(\text{uncoated})}$) values obtained for the uncoated nude manikin. Assuming that h_c for the aluminum-foil-coated segment equals h_c for the uncoated segment, h_r for the uncoated segment can be calculated as follows:

$$h_{r(\text{uncoated})} - h_{r(\text{foil})} = h_{r(\text{uncoated})} - h_{r(\text{foil})}$$

$$h_{r(\text{foil})} = \frac{0.1}{0.95} h_{r(\text{uncoated})}$$

$$h_{r(\text{uncoated})} \left(1 - \frac{0.1}{0.95}\right) = h_{r(\text{uncoated})} - h_{r(\text{foil})}$$

$$h_{r(\text{uncoated})} = 1.12(h_{r(\text{uncoated})} - h_{r(\text{foil})}) \quad (\text{W/m}^2 \text{ per K})$$

The calculations were performed using manikin measurements taken in still air within the controlled environment chamber at UC Berkeley, in both the standing and seated positions. Mean air temperature was equal to mean radiant temperature and both were uniform throughout the vertical extent of the manikin's occupied zone. Only one leg and arm was foiled at a time so that the foiled segment's surrounding radiant field would include the normal radiant contribution of the other.

Estimation of convective heat transfer coefficients

Subtraction of h_r from the total dry heat transfer coefficients, h , of the uncoated manikin, gives the convective heat transfer coefficients, h_c . Convective heat transfer coefficients were thus obtained for the manikin, in both standing and seated posture, under eight wind directions (0 to 315 azimuth degrees in 45° increments). Seven individual wind speeds were tested for each posture and direction to enable regression curves to be fitted to the h_c results, giving 112 experiments in total. A convective heat transfer coefficient was derived for each of the 16 manikin body segments in each of the 112 experiments.

Procedure

The wind tunnel tests were performed in the following sequence. The manikin was positioned facing upwind (azimuth angle 0°), its heating circuits were turned on and the instrument brought to ther-

mal equilibrium under still-air conditions. This provided a check on manikin operation before proceeding with each experiment. Once the whole-body value of boundary layer thermal resistance under still air conditions (I_a) fell within the benchmark values established in the climate chamber (whole-body resistance in the range of 0.116 W/m^2 per K $< I_a < 0.132 \text{ W/m}^2$ per K), the wind tunnel's fan was turned on and adjusted until the desired air speed ($\pm 0.05 \text{ m/s}$) was recorded within the manikin's occupied zone. The manikin was then equilibrated to the controlled wind speed with an azimuth angle of 0°, which typically required between 1 and 2 h for the first measurement of the day. Manikin segment temperatures and power inputs were logged for at least 10 min after equilibration, with logger scans every 120 s. All subsequent h_c calculations were based on the last five scans within each log file, which coincided with both the measurements of the wind tunnel's air speed and operative temperature profiles. Once all data for the 0° wind azimuth had been collected, the manikin was reoriented to the second azimuth position. Thermal equilibrium for this and the remaining seven wind directions was established within approx. 30 min.

Experiments involving the manikin in the fully erect posture required a slight departure from the procedure described above. Originally designed for architectural scale model work, the wind tunnel's working area dimensions did not allow the thermal manikin to stand fully erect. Therefore, experiments for the standing posture were performed by slightly bending the manikin's legs at the knees. These experiments had to be performed twice to allow both upper and lower leg segments each to be measured in the vertical position. The final set of data for the standing posture experiments were therefore composites of all vertical body segments from two separate wind tunnel runs.

Table 5 Body segment radiative heat transfer coefficients (h_r) for the nude thermal manikin ($\epsilon=0.95$)

Manikin segment	Seated h_r (W/m^2 per K)	Standing h_r (W/m^2 per K)
Foot (l and r)	4.2	3.9
Lower leg (l and r)	5.4	5.3
Thigh (l and r)	4.6	4.3
Pelvic region	4.8	4.2
Head	3.9	4.1
Hand (l and r)	3.9	4.1
Forearm (l and r)	5.2	4.9
Upper arm (l and r)	4.8	5.2
Chest	3.4	4.5
Back	4.6	4.4
Whole body	4.5	4.5

Table 6 Natural convective heat transfer coefficients (h_c) for the nude thermal manikin standing and sitting in still air ($v < 0.10 \text{ m/s}$)

Manikin segment	Seated natural convective h_c (W/m^2 per K)	Standing natural convective h_c (W/m^2 per K)
Foot (l and r)	4.2	5.1
Lower leg (l and r)	4.0	4.1
Thigh (l and r)	3.7	4.1
Pelvic region	2.8	3.4
Head	3.7	3.6
Hand (l and r)	4.5	4.1
Forearm (l and r)	3.8	3.7
Upper arm (l and r)	3.4	2.9
Chest	3.0	3.0
Back	2.6	2.9
Whole body	3.3	3.4

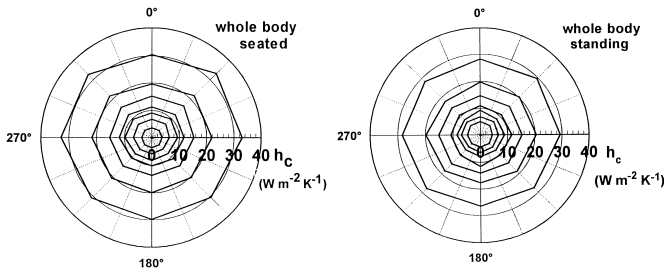


Fig. 4 The effects of wind direction on whole-body convective heat transfer coefficients for seated and standing postures. The seven curves in each graph represent the seven wind speeds under investigation: $v=0.2, 0.5, 0.8, 1.2, 2.0, 3.0$ and 5.0 m/s

Results

Individual body segments’ radiative heat transfer coefficients (h_r)

Values of h_r determined for each of the 16 manikin segments in the climate chamber are listed in Table 5. Values generally range between 4 and 6 W/m² per K. The whole-body h_r derived by weighting each estimate in Table 5 with the corresponding body segment surface area (Fig. 2) amounted to 4.5 W/m² per K for both the seated and the standing manikin.

Natural convection heat transfer coefficients (h_c)

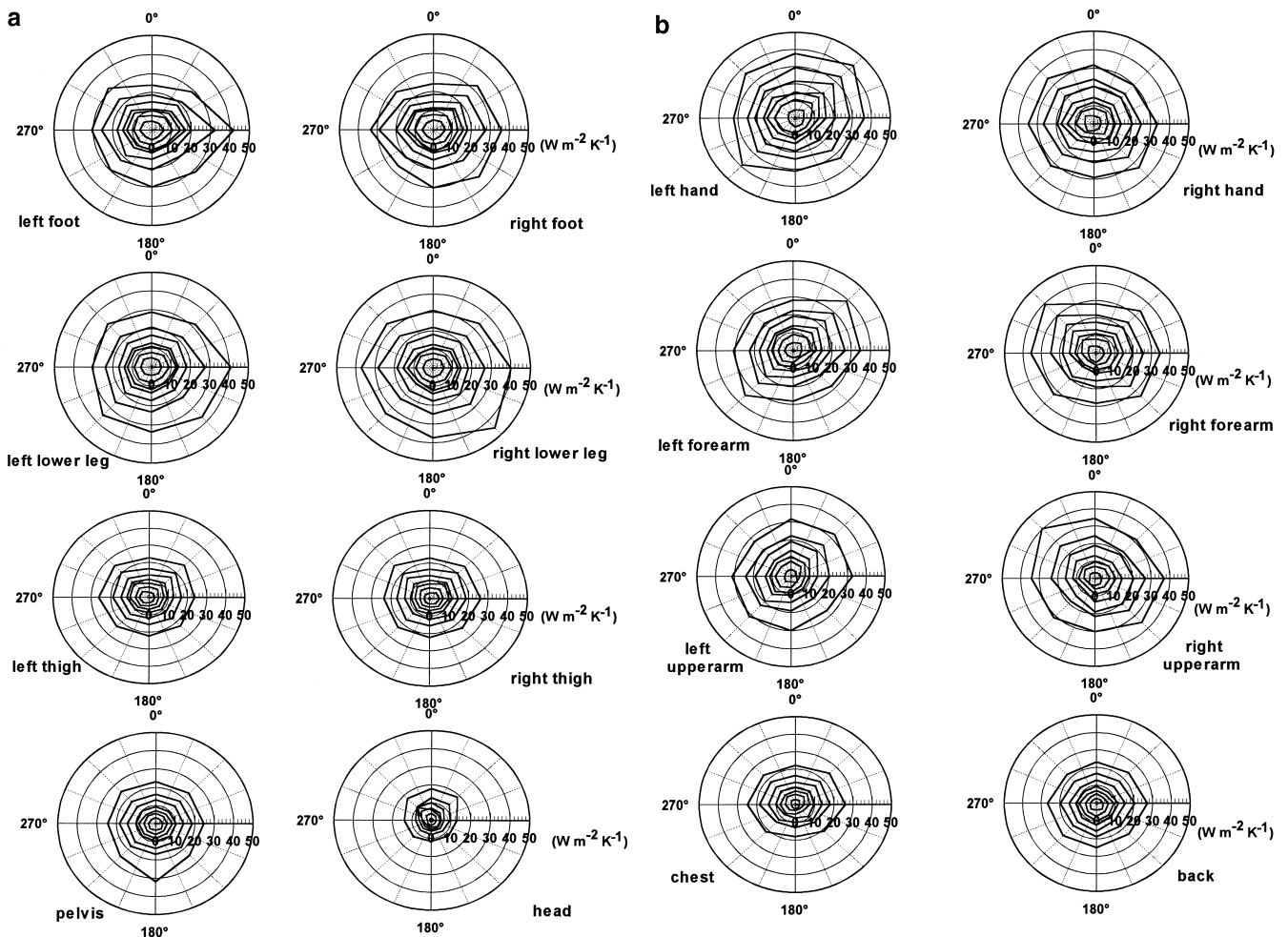
The natural convective heat transfer coefficients for each of the 16 body segments are listed in Table 6. These coefficients were calculated from data collected with the climate chamber’s air temperature 12 K cooler than the manikin’s mean skin temperature. The whole-body natural convection h_c , derived by weighting each estimate in Table 6 with the corresponding body segment surface area (Fig. 2) expressed as a fraction of whole-body surface area, amounted to 3.4 W/m² per K in the case of the standing manikin and 3.3 W/m² per K in the seated posture.

Convective heat transfer coefficients (h_c) in mixed and forced convective regimes

Effects of wind direction

The calculated whole-body h_c for eight wind directions and seven speeds are presented graphically in Fig. 4. Generally the pattern is one of uniform convection re-

Fig. 5a, b Effects of wind direction on convective heat transfer coefficients for individual body segments of a seated manikin exposed to wind speeds of $v=0.2, 0.5, 0.8, 1.2, 2.0, 3.0$ and 5 m/s



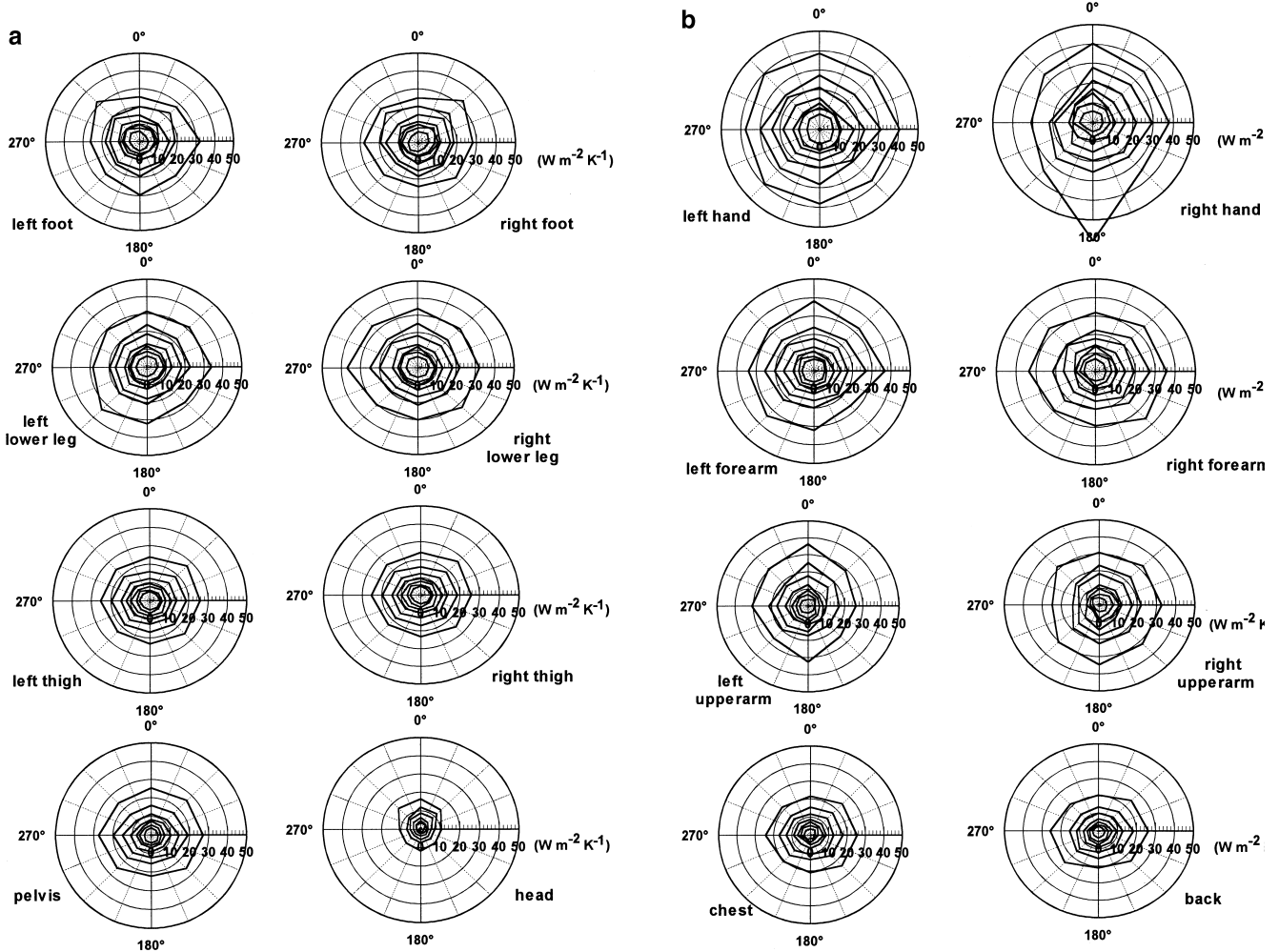


Fig. 6a, b Effects of wind direction on convective heat transfer coefficients for individual body segments of a standing manikin exposed wind speeds of $v=0.2, 0.5, 0.8, 1.2, 2.0, 3.0$ and 5 m/s

regardless of wind direction, although in the case of the seated subject, h_c is up to 10% higher for wind projected onto the manikin from the sides or the front diagonals. This effect becomes negligible at wind speeds of <0.8 m/s, which might be regarded as the practical upper limit of air speed for indoor environments intended for human occupancy (ASHRAE 1992).

In Fig. 5a and b are shown the convective heat transfer coefficients, h_c , of individual body segments plotted as a function of the azimuth angle of wind approach towards the seated manikin. Figure 6a and 6b depict the same data for the manikin in the standing position. The seven curves presented in each of the panels in Figs. 5 and 6 correspond to the seven wind speeds studied ($v=0.2, 0.5, 0.8, 1.2, 2.0, 3.0$ and 5.0 m/s). As seen in Fig. 5a, the feet and lower legs of the seated manikin experienced up to 30% higher overall convective heat loss for wind approaching from the side compared to front or back, but this directional effect was less pronounced in the standing posture (Fig. 6a). The standing manikin's right hand (Fig. 6b) experienced stronger convective heat loss for winds approaching from in front or behind. Both

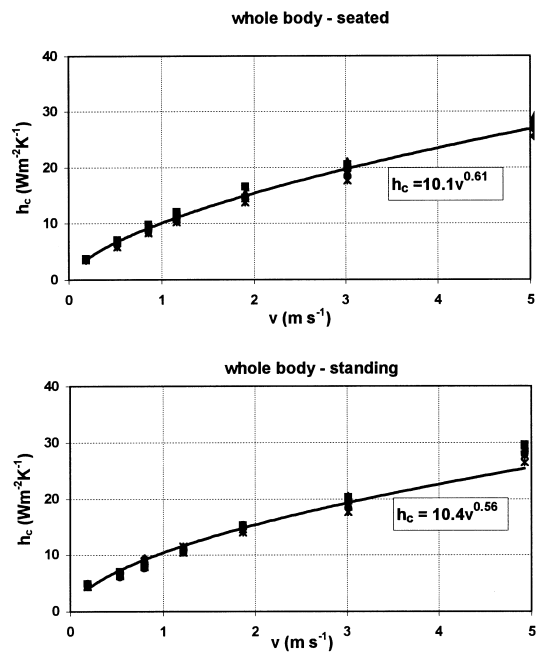


Fig. 7 Convective heat transfer regression models for the whole body, in seated and standing positions

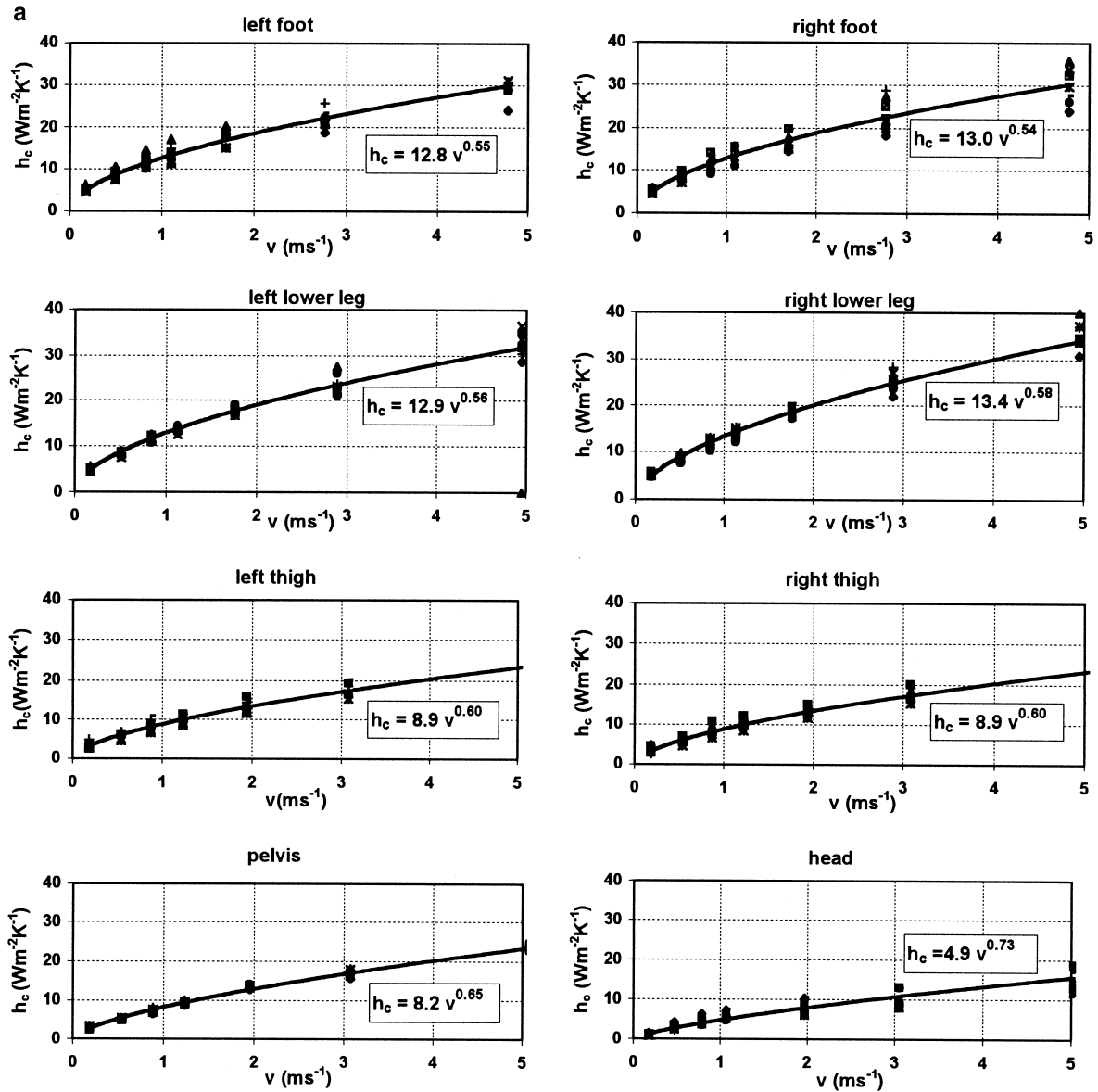


Fig. 8a, b Regression equations for the dependence of convective heat transfer coefficient (h_c) on air speed (v) for each of the seated manikin's body segments. Symbols represent the different directions tested

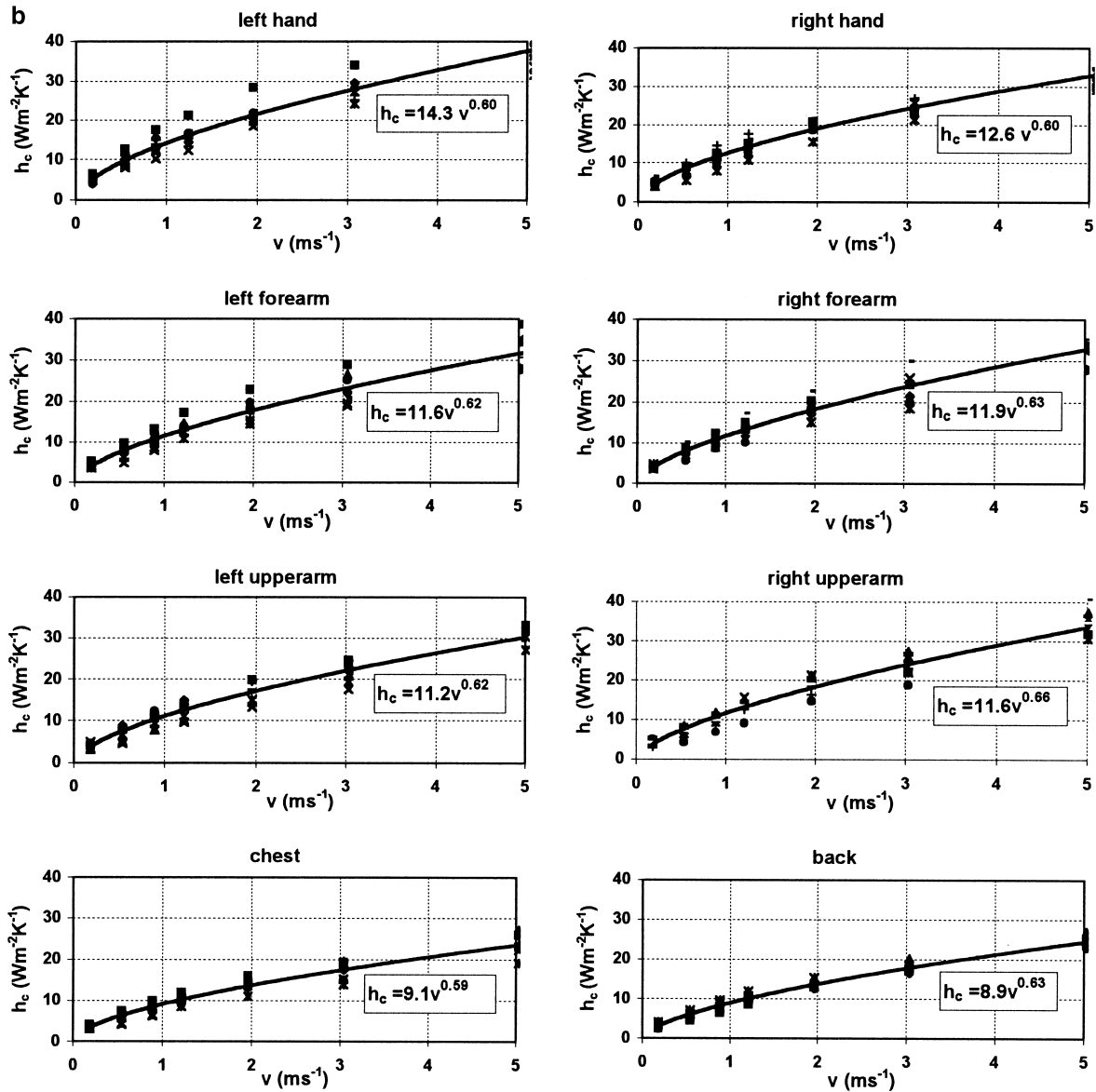
left and right forearms and upper arms showed between 20 and 30% higher convective losses when the wind had a diagonal azimuth approach angle, but this effect was evident only in the case of the seated manikin (Fig. 5b).

In the case of the standing manikin (Fig. 6b), with the arms hanging directly down beside the torso, convective losses were significantly diminished ($\leq 20\%$) when wind trajectories traversed the torso before reaching the arm (i.e. from the right in the case of the left upper arm and from the left in the case of the right upper arm). This directionality was absent in the case of the seated manikin (Fig. 5b), probably because the arms were tilted slightly forward and away from the vertical, which directly exposed them to the wind from both sides. Both chest and

back, in seated (Fig. 5b) and standing postures (Fig. 6b), experienced $\leq 10\%$ greater convective heat loss in winds approaching from the sides instead of the front or back. Of all 16 body segments under analysis, the head experienced the lowest convective heat loss in both seated and standing positions. However, significantly larger h_c values ($>50\%$) were obtained when the wind blew directly onto the face (Figs. 5a and 6a). These findings can probably be attributed to the thermal insulation afforded by the manikin's shoulder-length hair and the fact that her hair style left the face and neck entirely exposed from the front, but partly shielded from the sides and back.

Regression models of h_c on v

The seven wind speeds used in this study were selected to enable statistical relationships to be established for the dependence of h_c on air speed. Figure 7 portrays the rela-



relationship of whole-body h_c to air speed. The data of Figure 8a and b show the dependence of h_c on air speed for each of the 16 body segments with the manikin in the seated position; Fig. 9a and b similarly presents the data for the standing posture. Since the polar-plots of Figs. 5a to 6b indicate that wind direction exerted a minor effect on most of the body segments, only one power regression model is presented for each segment. The statistically derived model is based on h_c averaged across all eight wind directions, and has the general form:

$$h_c = Bv^n \quad (\text{W/m}^2 \text{ per K})$$

The whole-body regression models in Fig. 7 indicate a similar coefficient, B for both seated and standing postures, but the exponent n is $\approx 10\%$ higher in the case of the seated manikin, probably reflecting the slightly more exposed posture when seated. The net effect, however, is negligible at indoor design speeds (< 0.8 m/s). For individual body segments, all the regression models are highly

significant for the seated manikin, as indicated by the extent to which they account for the variance (r^2) in h_c . For 15 of the 16 body segments, the value of r^2 was $> 99\%$. The only exception is the manikin's head (r^2 of 97%).

As seen in Fig. 8a and b, the regression coefficient, B , in the 12 body limb segments (forearms, upper arms, hands, thighs, lower legs and feet) generally ranges between 10 and 14, with the only exception being the thighs, which are lower. Regression coefficients for central body segments such as pelvis, back and chest are generally lower than the limbs, the values ranging between 8 and 9. The lowest regression coefficient is registered by the head (including hair), at 4.9. The regression model exponent, n , fitted to regression models of the seated manikin's 16 body segments' convective heat transfer ranges between 0.54 and 0.66, with the only exception being the head (including hair), with $n=0.73$.

The data presented in Fig. 9a and b repeat the analysis described above, but for the manikin in the standing

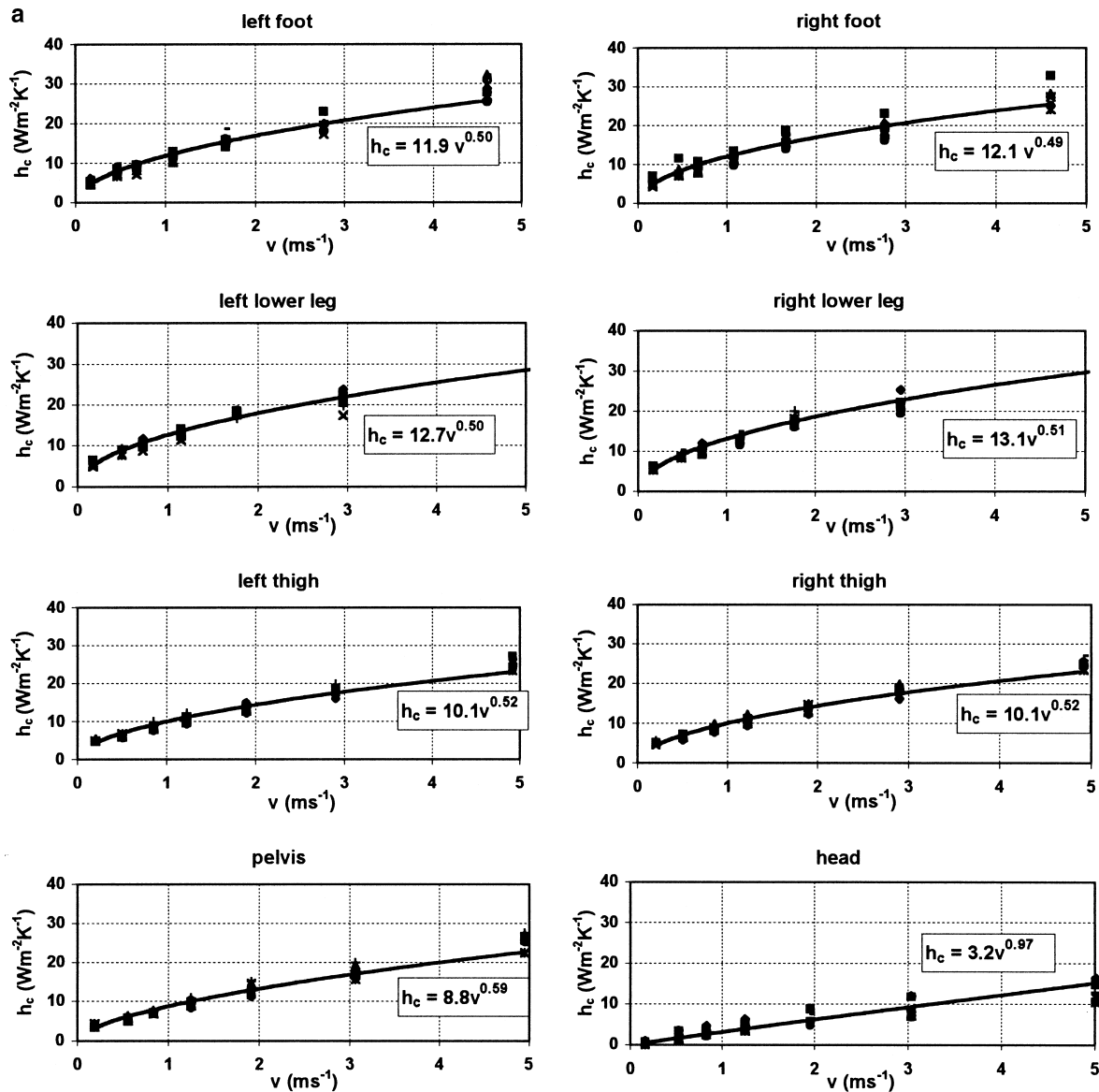


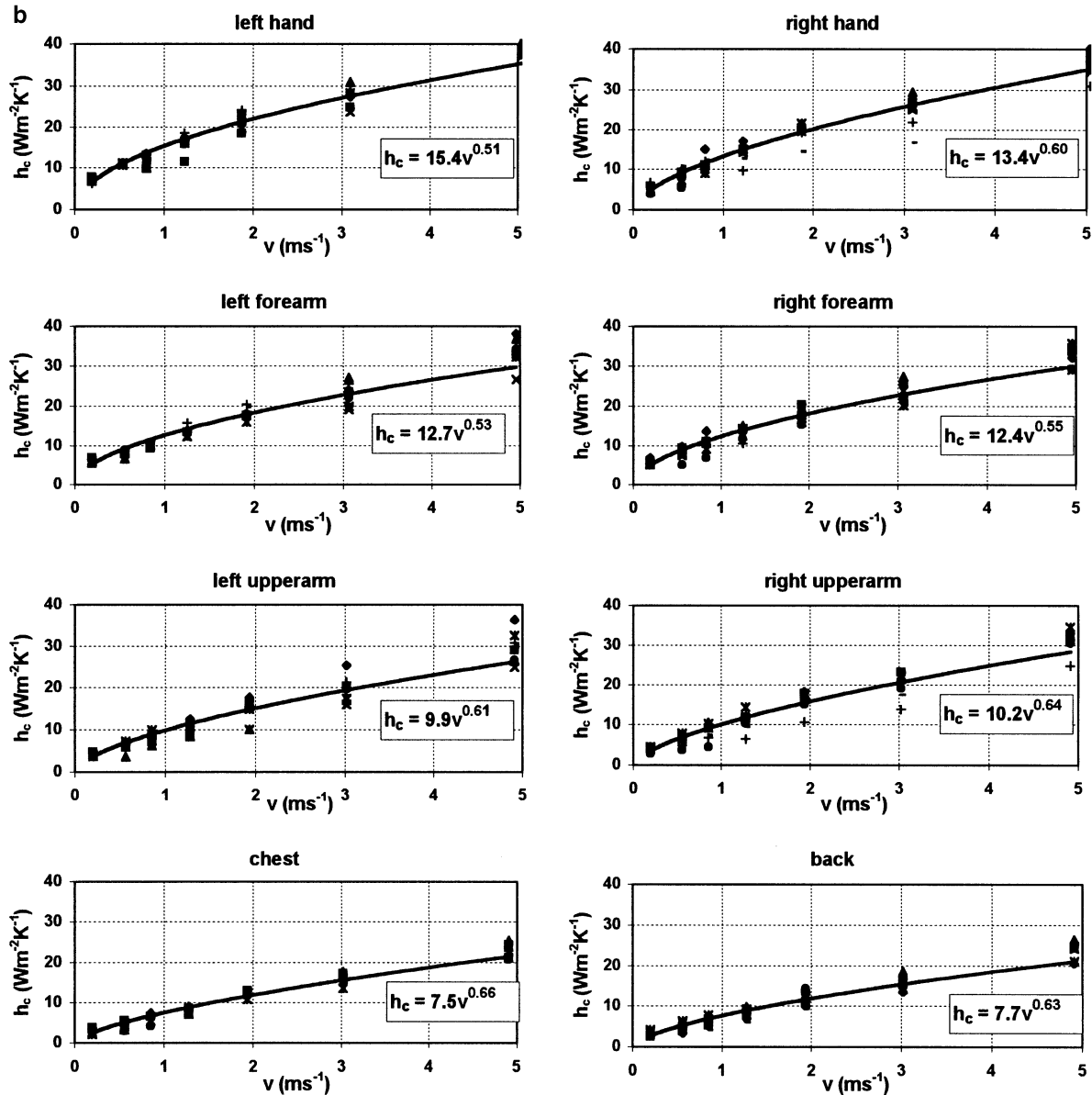
Fig. 9a, b Regression equations for the dependence of convective heat transfer coefficient (h_c) on air speed (v) for each of the standing manikin's body segments. Symbols represent the different directions tested

posture. Again the regression model in each graph is based on h_c values averaged across all eight wind directions. As in the case of the seated position, all regression models are highly significant ($r^2 > 97\%$ for all 16 segments). The regression coefficient, B , in the 12 body limb segments (forearms, upper arms, hands, thighs, lower legs and feet) range between 10 and 15, while the coefficients for torso segments (pelvis, back and chest) are lower, ranging between 7 and 9. The smallest convective heat transfer takes place from the head (including hair), with an almost linear regression of h_c on v [regression coefficient $3.2(\text{W/m}^2 \text{ per K})/(\text{m/s})$].

Discussion

Radiative heat transfer coefficients

The estimated sitting and standing values of h_r in this study ($4.5 \text{ W/m}^2 \text{ per K}$) closely match the whole-body, unspecified posture, value of $h_r = 4.7 \text{ W/m}^2 \text{ per K}$ published in Chapter 8 of the ASHRAE Handbook of Fundamentals (1993). This close agreement with the widely accepted value for whole body endorses our approach of applying aluminum foil to the surface of the manikin to partition dry heat transfer into its convective and radiative components. Furthermore, this agreement lends support for the segment-by-segment estimates of h_r and h_c obtained in this work. The sitting posture is normally regarded as having a smaller effective radiative area than the standing position, and therefore a smaller h_r would be expected for the seated manikin. The finding that h_r was the same for seated and standing may reflect the fact



that limbs are spaced further apart from each other and the torso when the manikin is seated. For example, the knees are approx. 0.30 m apart when seated, but no more than 0.05 m when in the standing position.

Natural convective heat transfer coefficients

The measured values for the whole-body natural convection coefficient are 3.3 and 3.4 W/m² per K for the seated and standing postures respectively. The present results for natural convective heat transfer coefficients are significantly lower than the 4.4 W/m² per K estimated by Fanger's (1970) PMV model for the same skin-to-air temperature gradient of 12 K used during the present manikin tests. Fanger's method was based on studies with human subjects in seated and standing positions. The present results are, however, consistent with the

range of 3.5 to 4.0 W/m² per K proposed by Danielsson (1993) for h_c at the surface of a loosely clothed subject standing in still air. Danielsson's estimates were based on the assumption that the mean natural convection coefficient for a vertical surface with constant heat flux occurs about half way up the characteristic length of the body, or at a height of ~0.7 m above the floor in the case of a human subject (Danielsson 1993). Applying the same generalization to the data obtained from a nude subject (comparable to the nude manikin of the present study), Danielsson (1993) estimated the standing whole-body natural convection coefficient to be 3.6 W/m² per K. The latter value is in good agreement with the present estimate of 3.4 W/m² per K, despite the fundamentally different methods used.

Table 7 Comparison between segment h_c equations^a from Ichihara et al. (1995) and the present study (standing position)

Manikin segment	Ichihara et al.		Present study	
	B	n	B	n
Feet	13.0	0.78	12.0	0.50
Lower legs	16.0	0.75	12.9	0.50
Back	17.0	0.50	7.7	0.63
Chest	11.0	0.67	7.5	0.66
Thighs	14.0	0.61	10.1	0.52
Upper arms	17.0	0.59	10.0	0.62
Forearms	17.0	0.61	12.5	0.54

^a Equations are of the general form $h_c = Bv^n$ (W/m² per K)

Comparison forced mode convection for different body segments

There was found to be a general tendency for convective heat losses to decrease from peripheral body segments such as feet and hands, towards the central segments of the torso such as chest, back and pelvis. At the highest air speeds investigated, the difference in h_c between hands and torso segments was approx. 40 to 60%, and this increased to >60% for lower air speeds typical of indoor conditions ($v < 0.8$ m/s). This observation underscores the errors involved when applying whole-body values of h_c such as those published in the ASHRAE Handbook of Fundamentals (ASHRAE 1993) in situations of highly non-uniform air flow. Such conditions would be typical in the context of environments such as task/ambient air-conditioned buildings, or in passenger cabins of vehicles, and it is recommended that the findings of the present research be adopted for such applications.

The h_c regression equations established for individual body segments in this study fall well below those published by Ichihara et al. (1995) for a standing manikin. While the areal dimensions of their manikin are not given and their manikin's segmentation differs from that of the present study, some exemplary comparisons between the two manikins for similar body segments are given in Table 7. Unfortunately Ichihara et al. (1995) offer insufficient details to enable explanations for these differences. However, it can be noted that their whole-body regression equation yields estimates for h_c consistently higher than those from any other equation included in ASHRAE's Handbook of Fundamentals (ASHRAE 1993) for motionless subjects in moving air (see Fig. 10). The whole-body h_c regression equation from Ichihara et al. (1995) is:

$$h_c = 15.4v^{0.63} \quad (\text{W/m}^2 \text{ per K})$$

Comparison of forced/mixed convection for different body postures

Comparing seated and standing postures in Fig. 7, the values of whole-body convective heat loss are slightly higher for the seated manikin. This postural effect may

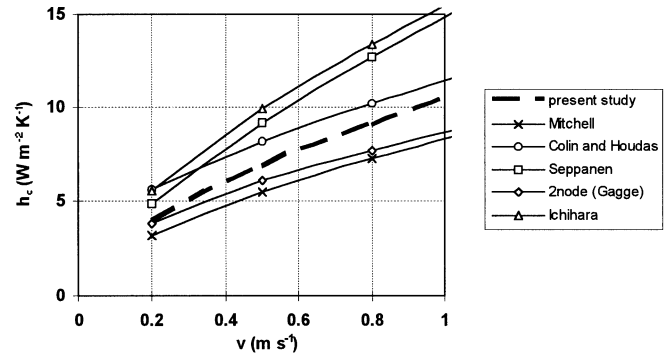


Fig. 10 Comparison of equations for convective heat transfer coefficients (h_c) cited in ASHRAE (1993) with the present study's whole-body equation (Ichihara et al. 1995; Gagge et al. 1986; Seppänen et al. 1972; Mitchell 1974; Colin and Houdas 1967)

result from the greater separation between limbs and torso, allowing freer air circulation around a greater body surface area, thus enhancing convective heat losses. However, at lower air speeds which might be representative of indoor conditions, the convective difference between postures becomes negligible. Therefore, in such situations with air speeds $0.2 < v < 0.8$ m/s, it is recommended that the following compromise regression function is suitable for general application indoors, regardless of posture:

$$h_c = 10.3v^{0.6} \quad (\text{W/m}^2 \text{ per K})$$

As seen in Fig. 10, the general purpose indoor h_c function falls in the middle of the range tabulated in ASHRAE's Handbook of Fundamentals (ASHRAE 1993, Chapter 8; cf. Table 6). The latter were selected as appropriate for motionless subjects in moving air. Admittedly this consensus may not formally validate the present study's methods, but at least encourages confidence in the segment-by-segment h_c findings presented here.

Effects of wind direction

The substantial effect of wind direction found in the Danielsson (1993) study of regional heat transfer coefficients is not supported by the present findings. This is probably due to the fundamentally different methods used in the two studies. Danielsson's (1993) convective heat transfer coefficients are based on spot measurements by heat flux plates located at various sites around the limb or segment in question, but with wind presented from a consistent direction throughout. The current data are integrated values from the entire segment surface area under different wind directions. In terms of applications, the current method is likely to be more relevant to the modelling requirements in task air-conditioning and other engineering applications. For example, predicting the thermal comfort implications of various options for air diffuser placement within an office workstation should proceed faster from a segment-by-segment rather than a spot-value heat-balance approach.

The unique and valuable feature of Danielsson's data, on the other hand, is the fact that they were collected on the surface of a clothed subject, as opposed to the nude measurements in the present paper. Clothing surface heat transfer is difficult to measure using the segment heat-balance method, and in our laboratory we are now only beginning to attempt to do this. Despite the methodological differences, the consistency between whole-body natural convection h_c measurements in both studies suggests that the combined effects of shape, folds, surface roughness and thickness of clothing on external surface h_c were negligible. This deduction encourages generalized of the results of the present study based on nude segment-by-segment estimation of h_c to situations with clothed subjects, at least until empirical data are established.

Conclusions

1. A thermal manikin with controlled skin temperature was used to analyse sensible heat transfer between body and environment under a variety of conditions representative of indoor and outdoor microclimates.
2. Application of a low emissivity, highly reflective film to the skin of the thermal manikin enabled partitioning of dry heat flux into its radiative and convective components.
3. Whole-body estimates of the radiative heat transfer coefficient, h_r , and the convective heat transfer coefficient, h_c , in both still and moving air, fell within the mid-range of estimates already published in the literature, suggesting that the methods used to estimate regional heat transfer coefficients are valid.
4. Hands, feet and peripheral limbs generally had higher convective heat transfer coefficients than the central torso region.
5. Heat transfer coefficients for the head and neck were the smallest of all body regions, reflecting the insulative properties of the manikin's shoulder-length hair.
6. For the two postures investigated in this paper, seated and standing, natural convective heat losses were similar in still air. However, in moving air, convective heat losses were slightly greater for the more open, seated posture.
7. Wind direction was a significant parameter for the heat balance of individual body segments in only a small number of cases, such as the feet and lower legs. These segments experienced higher convective heat losses whenever the wind approached from the left or right side of the body, and this directionality was only evident for the seated posture. Another example of significant wind direction effects was when the standing subject's arms were partially shielded from the approaching wind by the torso.

The present investigation suggests several avenues for useful further work. For example, the natural convection heat transfer coefficients in the present study were determined with a skin-to-air temperature gradient of ~ 12 K.

Since this is larger than normally encountered in most indoor situations, and since natural h_c is known to depend on this temperature gradient, future work should quantify the strength of the dependence to individual body segments under various postures.

While the present study covered all wind approach directions in the horizontal plane (azimuths), the use of a horizontal wind tunnel precluded extension of the investigation to wind elevation angles. Since overhead fans or ceiling-mounted air diffusers represent a common method of enhancing convective heat loss from the human body, a quantitative examination of this dimension represents a worthwhile future project. Such an experiment may involve the use of a vertical wind tunnel such that the natural buoyancy within the body's boundary layer operates along the same axis as the wind tunnel's forced convection. Furthermore, in view of the increasing popularity of floor-based task-conditioning systems, such an experiment should examine forced convection resulting from air flows delivered to the subject from below.

The present study was restricted to static manikin experiments. That is, the manikin remained stationary in either the seated or standing position for the duration of the experiment. A worthwhile extension might be to animate the manikin with a 'walking device' attached to its articulated limbs (Olesen et al. 1982; Chang et al. 1988). Such studies would enable the 'pendulum effect' (Clark and Edholm 1985) to be incorporated into the h_c regression models by expressing air speed relatively, as a sum of the speed of walking, running or cycling, and the air speed itself. The pendulum effect refers to the limbs of a moving subject swinging both with and against the general flow of air in quick succession, thereby cyclically decreasing and increasing the relative air speed and corresponding convective heat losses from the limb in question. The effect on heat transfer should become increasingly significant as the exercise intensifies, so application of the current regression equations for h_c in the context of athletic subjects is not recommended. Finally, heat transfer from clothed surfaces should be examined via the segment-by-segment approach under the influences of wind and body motion.

Acknowledgements Raelene Sheppard (Climatic Impacts Centre) helped with some of the data analysis. Adil Sharag-Eldin (CEDR) provided advice on the operation of the wind tunnel and measured the wind turbulence spectra. The Pacific Gas and Electric Company's Energy Center in San Francisco lent us an infrared thermovision system for these experiments. The research was partially funded by the California Institute for Energy Efficiency (CIEE), a research unit of the University of California. Publication of research results does not imply CIEE endorsement of or agreement with these findings, nor that of any CIEE sponsor.

References

- ASHRAE (1992) Indoor environmental conditions for human occupancy. ANSI/ASHRAE Standard 55. ASHRAE, Atlanta
- ASHRAE (1993) Physiological principles and thermal comfort. In: ASHRAE handbook of fundamentals. ASHRAE, Atlanta, pp 8.1–8.29

- Baumann FE, Zhang H, Arens EA, Benton C (1993) Localized comfort control with a desktop task conditioning system: laboratory and field measurements. *ASHRAE Trans* 99:733–749
- Chang SWK, Arens EA, Gonzalez RR (1988) Determination of the effect of walking on the forced convective heat transfer coefficient using an articulated manikin. *ASHRAE Trans* 94:71–81
- Clark JA, Edholm OG (1985) *Man and his thermal environment*. Edward Arnold, London
- Clark RP (1981) Human skin temperature and convective heat loss. In: Cena K, Clark JA (eds) *Bioengineering, thermal physiology and comfort*. Elsevier, Amsterdam, pp 57–76
- Clark RP, Toy N (1975) Natural convection around the human head. *J Appl Physiol* 244:283–293
- Colin J, Houdas Y (1967) Experimental determination of coefficient of heat exchange by convection of the human body. *J Appl Physiol* 22:31–38
- Danielsson U (1993) *Convection coefficients in clothing air layers*. Thesis, Royal Institute of Technology, Stockholm
- Fanger PO (1970) *thermal comfort*. Danish Technical Press, Copenhagen
- Gagge AP, Fobelets AP, Berglund LG (1986) A standard predictive index of human response to the thermal environment. *ASHRAE Trans* 92:709–731
- Heinemeier KE, Schiller GE, Benton CC (1990) Task conditioning for the workplace: issues and challenges. *ASHRAE Trans*, 96:678–688
- Houdas Y (1981) Modelling of heat transfer in man. In: Cena K, Clark JA (eds) *Bioengineering, thermal physiology and comfort*. Elsevier, Amsterdam, pp 111–120
- Ichihara M, Saitou M, Tanabe S, Nishimura M (1995) Measurement of convective heat transfer coefficient and radiative heat transfer coefficient of standing human body by using thermal manikin. *Proceedings of the Annual Meeting of the Architectural Institute of Japan*, pp 379–380 (in Japanese)
- Kerslake DMcK (1972) *The stress of hot environments*. Cambridge University Press, Cambridge, UK
- Mayer E (1992) New measurements of the convective heat transfer coefficient: influence of turbulence, mean air velocity and geometry of the human body. In: *Roomvent '92 (Third International Conference)* Aalborg, pp 263–276
- McIntyre DA (1980) *Indoor climate*. Applied Science Publishers, London
- Mitchell D (1974) Convective heat loss in man and other animals. In: Montieth JL, Mount LE (eds) *Heat loss from animals and man: assessment and control*. Butterworths, London
- Nishi Y, Gagge AP (1970) Direct evaluation of convective heat transfer coefficient by naphthalene sublimation. *ASHRAE Trans* 29:830–838
- Olesen BW, Sliwiska E, Madsen TL, Fanger PO (1982) Effects of body posture and activity on the thermal insulation of clothing, measured on a moveable thermal manikin. *ASHRAE Trans* 88:791–805
- Oke T (1987) *Boundary layer climates*. Methuen, London
- Seppänen O, McNall PE, Munson DM, Sprague CH (1972) thermal insulating values for typical indoor clothing ensembles. *ASHRAE Trans* 78:120–130
- Stolwijk JAJ (1970) Mathematical model of human thermoregulation. In: Hardy JD, Gagge AP, Stolwijk JAJ (eds) *Physiological and behavioral thermoregulation*. Thomas, Springfield, pp 703–721
- Tanabe S, Arens EA, Bauman FS, Zhang H, Madsen TL (1994) Evaluating thermal environments using a thermal manikin with controlled surface skin temperature. *ASHRAE Trans*, 100:39–48
- Test FL, Lessman RC, Johary A (1981) Heat transfer during wind flow over regular bodies in the natural environment. *J Heat Transfer* 103:262–267
- Winslow C-EA, Gagge AP, Herrington LP (1939) The influence of air movement on heat losses from the clothed human body. *J Physiol* 127:505–515
- Wissler EH (1970) Comparison of results obtained from two mathematical models – a simple 14 node model and a complex 250-node model. *J Physiol (Paris)* 63:455–458
- Wyon DP (1989) Use of thermal manikins in environmental ergonomics. *Scand J Environ Health* 15 (Suppl 1):84–94